Limitations of the State of Health and Health Indicators for Electric Vehicle batteries

Maite Etxandi-Santolaya
Energy Systems Analytics Group
Catalonia Institute for Energy Research - IREC
Barcelona, Spain
metxandi@irec.cat

Lluc Canals Casals
Dept of Engineering Projects and Construction
Universitat Politècnica de Catalunya - UPC
Barcelona, Spain
lluc.canals@upc.edu

Cristina Corchero
Energy Systems Analytics Group
Catalonia Institute for Energy Research - IREC
Barcelona, Spain
ccorchero@irec.cat

***Abstract*—Estimating the State of Health of Electric Vehicle batteries is a crucial yet challenging task. Various Health Indicators have been proposed to assess degradation, yet several of them may not be obtainable under normal operation. Additionally, battery degradation alone does not provide insights into the battery's functionality for a specific application. To address these limitations, this study analyses experimental data reflecting diverse driving conditions and evaluates the efficacy of various Health Indicators to estimate the State of Health. Results show that the value of the second peak in the Incremental Capacity curve and the use of multiple indicators produce the most accurate results. Furthermore, this study introduces a functional definition of battery degradation through the State of Function, which combines the specific driving requirements with the capacity to estimate how far the battery is from its functional End of Life. This approach provides a more comprehensive understanding of the battery's health and its ability to perform efficiently for a given application.**

***Index Terms*—Electric Vehicle battery, Health Indicators, State of Function, State of Health**

I. Introduction

The transition to electric mobility is driven by the need to decrease greenhouse gas emissions, combat climate change, and improve air quality [1]. To promote Electric Vehicle (EV) adoption, governments are implementing policies and incentives, while car manufacturers are transitioning to electric models [2]. As a result, the number of EVs on the road is expected to grow significantly in the near future [3].

Despite significant advances in EV research, further technological improvements are necessary to enhance their practicality, efficiency, and sustainability. A crucial issue in this regard is related to the estimation of battery degradation, which is the gradual loss of usable capacity and power [4]. To improve battery monitoring and control and prevent compromising the driving experience, efforts are being invested in predicting the State of Health (SoH), which measures battery degradation.

Health Indicators (HI) can be extracted from a snapshot of battery performance, typically from the temperature, current, and/or voltage curves [5]. Several HIs have been obtained in the literature that show a strong correlation with the SoH. These HIs are mostly derived from the Constant Current (CC) - Constant Voltage (CV) charge period, which provides more stable conditions than during driving [6]. Potential HIs derived from this period include the CC charge time [7]–[9], CC charge capacity or energy [9], [10], CV charge time [7], [9], CV charge capacity or energy [9], [10], proportion of CC time over total charge [8], [9] and the slopes at the end of the CC charge [6]. However, obtaining these HIs requires a full CC-CV charge, which is not commonly available on EV charges. Based on partial charges, the coefficient of variation of the current during CV and the coefficient of variation of the voltage during CC has been proposed [11]. Another set of HIs is the time for Equal Voltage Increase (EVI), which calculates the time that it takes to reach a specific voltage jump [12]. Similarly, the voltage change during Equal Time Increase (ETI) [9] can be considered. For EVIs and ETIs to be effective, the voltage ranges used must be common in the user's charging pattern. Additionally, HIs based on the minimum, maximum or mean temperatures and the area under the curves during CC and CV charges have been suggested [9]. Nonetheless, the results may be distorted by the impact of cooling and variations in ambient temperature.

An important set of HIs during charge are the ones derived from the Incremental Capacity Analysis (ICA) [13]. Incremental Capacity (IC) curves convert the plateau region of the Voltage-Capacity curve into identifiable peaks that provide insight into the degradation mechanisms [14]. Several HIs can be extracted from these curves, like the peak location, the peak value or the area under the peaks [8], [9], [15]. However, these curves are sensitive to the value of the c-rate [16] and temperature and many of the SoH algorithms proposed through this approach assume a full charge [17], discarding the variation of the curves depending on the voltage range. Similarly to the ICA, the Differential Voltage Analysis (DVA) can be considered which represents the differential voltage over the charge throughput [18].

Other HIs can be derived from the discharge period. Similarly to the ones obtained during the charge, the time for a full CC discharge is employed as a HI [19]. Considering that full discharges are not available onboard, the equal voltage decrease time [8], [19], [20] or the energy [10] can be defined during a CC discharge between the desired voltages. Nevertheless, HIs obtained in this way are not realistic for EVs, as the current rarely remains constant during driving.

HIs extracted from the rest periods can also be considered. For example, the voltage recovery of the battery after the EV stops has been proposed [21]. Another work used the relaxation voltage after a full charge and 30 minutes of rest [22].

Finally, other studies employ the Internal Resistance (IR) as a HI for a capacity-based SoH [7], [15], [19]. However, since decreased capacity and increased IR can have distinct implications for performance, it is recommended to estimate both variables independently.

Selecting the most adequate HIs among the existing ones, requires a comparative study of their accuracy and usefulness for on-board algorithms. In this sense, a recent review evaluated the practicality and complexity of several HIs for online SoH predictions, but it was limited to discussing different approaches and did not include experimental data [17]. Another study conducted laboratory experiments with an LFP cell to determine a large number of HIs and their correlation with SoH using grey relation analysis [6]. However, the cell was cycled based on a battery storage system profile rather than an EV, and the testing of only one cell did not allow for evaluating how different operating conditions might affect the HI value for the same SoH.

After selecting one or more HIs, linear regression [15] or more complex machine learning algorithms (e.g. Gaussian Process Regression [11] or Neural Networks [12]) can be employed to estimate the SoH of a battery. However, this approach has a significant limitation: while the SoH provides valuable information, it lacks interpretability for a specific application. Because driving patterns and environmental conditions vary, the required functionalities of batteries differ for each driver [23]. To overcome this limitation, the State of Function (SoF) can be used. Following a previous work, the SoF can be defined to consider how far a battery is from becoming unusable for a particular application and reaching its end of life [24].

The aim of this study is to evaluate the performance of various HIs and define the SoF for different cases. Compared to previous studies that analysed HIs, this work employs realistic and varied cycling data. Laboratory experiments were conducted to six cells using profiles derived from real driving that represent different drivers, enabling the evaluation of the HIs for different usage patterns and estimate the SoH. As a key contribution, the specific driving requirements are compared to the degradation level to define the SoF and provide a useful indicator of the battery's functionality for each case.

II. Methodology

A. Experimental Set-up

The data for this study consists of the laboratory cycling performed to six 5Ah Li-ion cylindrical cells with NMC cathode from the manufacturer LG Chem, model INR21700M50LT. The equipment used to cycle the cells is the BaSyTec XCTS Mk II and the temperature is controlled with the climate chamber Arbin MZTC.

To simulate realistic driving conditions, synthetic driving profiles were generated using real data, as presented in a previous work [23]. The profiles are generated based on road type (Semi Urban (SU) or Semi Highway (SH)) and the duration of the driving trip. Data collected for over 1.5 years from 24 EVs and 3 different European regions is used to define the driving times that cover 50% and 90% of the trips. Instead of considering the same duration for each day, to add variability, the daily driving time is obtained from a normal distribution where the standard deviation is 5% of the average. Table I shows the road type, population covered, average trip duration between charges and battery capacity considered for each of the six cells. After each driving trip, the cell is charged with a constant current of C/3. The cycling was first performed at ambient temperature and then at 35ºC to accelerate the degradation. Therefore, each of the cells represent a different driver that uses the EV daily to perform relatively homogeneous trips and charges the battery everyday.

TABLE I: Description of the cycling for each cell

Cell	Road	Population covered	Av. driving time	Capacity
1	SH	50%	44 min	30 kWh
2	SH	50%	44 min	65 kWh
3	SH	90%	109 min	65 kWh
4	SU	50%	52 min	30 kWh
5	SU	50%	52 min	65 kWh
6	SU	90%	126 min	65 kWh

Reference Performance Test (RPT) are performed at 25ºC to evaluate the degradation and include a full CC-CV charge at C/3 rate and a full discharge at 1C, repeated twice.

B. Health Indicators

The criteria employed for selecting HIs for this study considers the following points:

- HIs that assume CC conditions during discharge are not considered due to their unrealistic nature.
- Temperature related HIs are not considered as they neglect the effect of the cooling system.
- DVAs based HIs are not consider as they contain similar information as ICA based ones, which are considered.
- HIs that cannot be obtained from the available data are not considered. This includes the voltage relaxation, as no rest period was considered after the driving cycles.
- Since the IR is more useful decoupled from the capacity fade, it is not considered as a HI.

Table II summarizes the HIs obtained from the full charges of the RPTs, as shown in Fig 1. The equations for the slope HIs, EVI, ETI are shown below. $Vmax$, $Vmin$ and dt depend on the range, as specified in Table II.

$$Slope = \frac{Vmax - Vmin}{t_{Vmax} - t_{Vmin}} \tag{1}$$

$$EVI = t_{Vmax} - t_{Vmin} \tag{2}$$

$$ETI = V_{CCend} - V_{CCend-dt} \tag{3}$$

The IC curve is obtained from Equation 4, where dV is 15mV. IC_V and IC_P are obtained by locating the peaks and the area is calculated using Equation 5 which considers the adjacent points to the peak.

$$IC = \frac{dQ}{dV} = \frac{Q_t - Q_{t-1}}{V_t - V_{t-1}} \tag{4}$$

$$IC_A = (V_{P+1} - V_{P-1})(\frac{Q_{P+1} + Q_{P-1}}{2}) \tag{5}$$

C. State of Health algorithms and error definition

Once the HIs are obtained, the next step is to develop a SoH algorithm. To accomplish this, the data containing the HIs for each charge is split into train and test sets, with the former containing 80% of the data. Random data points for all available cells are included in the train dataset, which is used to build the SoH algorithms. Equation 6 shows the regression used to estimate the SoH.

$$SoH = a + \sum_{i=1}^{n} b_i HI_i \tag{6}$$

TABLE II: Health Indicators employed

Health Indicator		Label
CC Time		t_{CC}
CC Capacity		Ah_{CC}
CC Time Ratio		$t_{CC/total}$
CV Time		t_{CV}
CV Capacity		Ah_{CV}
Slopes at CC charge end	3.4-3.6V	$SlopeCC_1$
	3.6-3.8V	$SlopeCC_2$
	3.8-4V	$SlopeCC_3$
	4-4.2V	$SlopeCC_4$
EVI	2.6-3V	EVI_1
	3-3.4V	EVI_2
	3.4-3.8V	EVI_3
	3.8-4.2V	EVI_4
ETI	Last minute of CC charge	ETI_1
	Last 5 mins of CC charge	ETI_2
	Last 10 mins of CC charge	ETI_3
ICA	Peak 1 Voltage	IC_{V1}
	Peak 1 Value	IC_{P1}
	Peak 1 Area	IC_{A1}
	Peak 2 Voltage	IC_{V2}
	Peak 2 Value	IC_{P2}
	Peak 2 Area	IC_{A2}
	Peak 3 Voltage	IC_{V3}
	Peak 3 Value	IC_{P3}
	Peak 3 Area	IC_{A3}
	Peak 4 Voltage	IC_{V4}
	Peak 4 Value	IC_{P4}
	Peak 4 Area	IC_{A4}

D. State of Function definition

As previously discussed, the SoF can be used to relate the degradation with the driving requirements. In this study, the SoF considered is limited to the capacity aspects (SoF_e) and future work will integrate power related considerations. The SoF_e is defined by Equation 7 where E_{EoL} and E_{BoL} denote the End of Life (EoL) and Beginning of Life (BoL) capacities in kWh, respectively [25].

$$SoF_e = \frac{(E_{BoL}\, SoH) - E_{EoL}}{E_{BoL} - E_{EoL}} \tag{7}$$

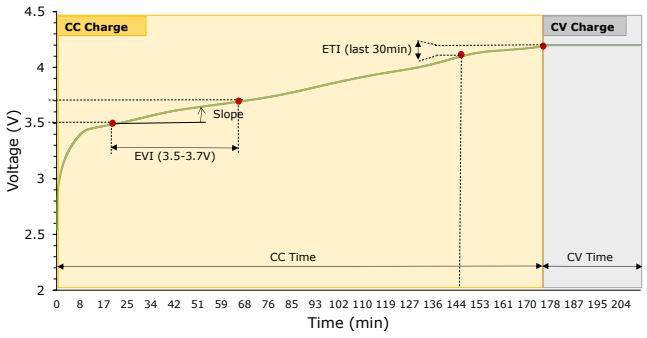

(a) Voltage during CC-CV charge

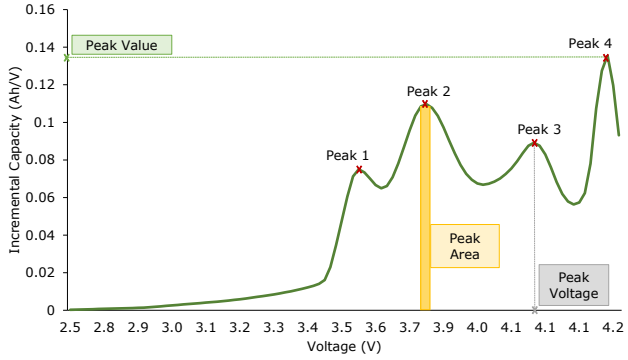

(b) Incremental Capacity curve

Fig. 1: Health Indicators during CC-CV charge

The definition of E_{EoL} is done considering that the battery reaches the EoL once it is not able to provide 95% of the driving trips of the user. The E_{EoL} values are 6.48 kWh (Cell 1 and 2), 21.19 kWh (Cell 3), 5.03 kWh (Cell 4 and 5) and 15.56 kWh (Cell 6). It is noteworthy that some cases have the same EoL requirement since only the nominal battery capacity is changed, and the driving considered is the same.

III. Results

First the HIs corresponding to the full RPT charges are presented. The left side of Fig 2 displays the Spearman correlation values for all the HIs considered. A sub-selection of HIs with a correlation greater than 0.75 is then obtained, which are, in order of correlation, IC_{P2}, t_{CC}, Ah_CC, IC_{A2}, EVI_3, $SlopeCC_2$ and $SlopeCC_1$. The right side of Fig 2 shows the correlation matrix of the HIs and the SoH. Since Ah_{CC} shows the same values as t_{CC}, it is no longer considered.

Fig 3 represents the CC-CV and IC curves for various degradation levels, including zoomed-in views of the voltage ranges (3.4-3.8V) relevant to the selected HIs. Note that visualizing the degradation trend in the CC-CV curve is not straightforward. In fact, the IC curve is introduced to help identify movements more clearly. As the Spearman correlation confirms, the second peak in the IC curve exhibits a clear tendency with degradation. As the battery ages, the peak value (IC_{P2}) and the area under the peak (IC_{A2}) decrease. In terms of voltage-related HIs, EVI_3 shows a decreasing trend with the SoH, while both slopes ($SlopeCC_2$ and $SlopeCC_1$) appear to increase as the battery ages. Finally, the time during the CC period (t_{CC}) decreases with degradation.

The HIs that show the highest correlation are used to build a regression-based SoH algorithm following Equation 6 (n=1). The regression for each HI is depicted in Fig 4. The black line represents the regression results obtained by considering all datapoints, while the other lines represent regression obtained by considering the datapoints for each cell. Ideally, if a HI is independent of the cycling conditions, the trends for each cell should be similar.

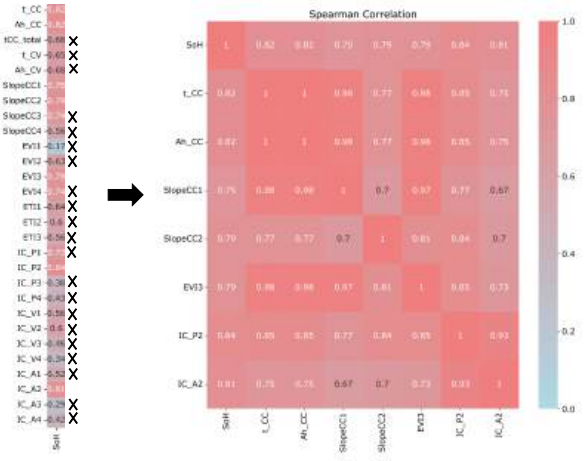

Fig. 2: HI selection based on Spearman correlation

Besides creating regressions for single HIs, combining them can enhance the performance of the estimation. All possible combinations of more than two HIs have been tested, and the combination that minimizes the errors contains IC_{P2}, t_{CC}, EVI_3, $SlopeCC_2$ and $SlopeCC_1$. This model is referred to as $multiHIs$ and follows Equation 6 (n=5).

Table III shows the MAE, the MSE and the $RMSE$ for each model. Results show that the $multiHIs$ model produces the smallest estimation error. In terms of the most accurate HI, all error metrics are the lowest when considering IC_{P2}.

Considering the EoL values presented in Section II-D, Fig 5 shows the measured SoH values translated to the SoF_e for each case. Although the SoH trends are comparable for all cells, the SoF_e differs from cell to cell. Cell 3 has the most restrictive capacity requirements and shows the fastest decrease in SoF_e, implying that it is likely to reach EoL

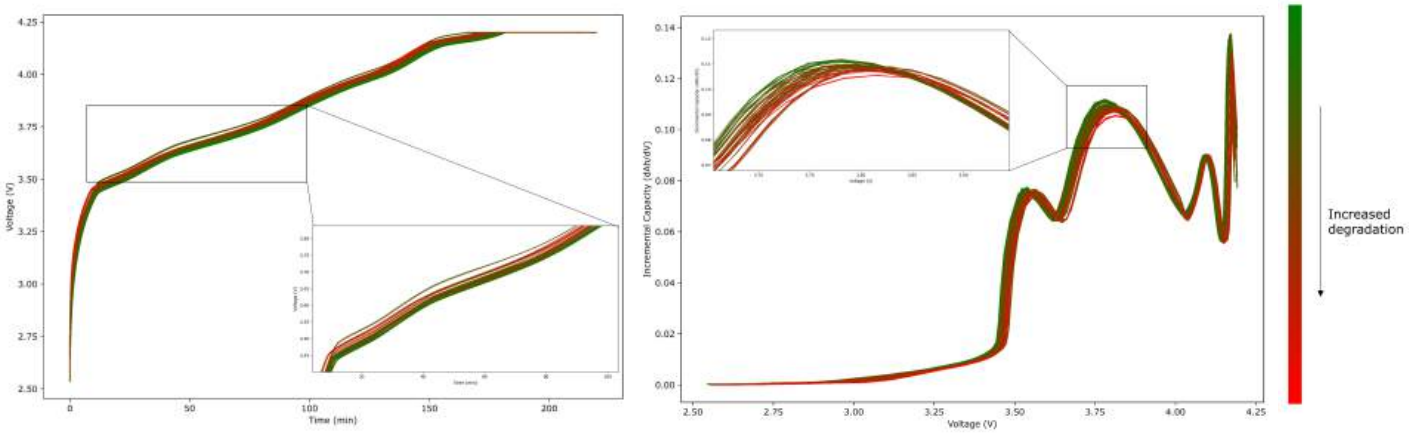

(a) Voltage during CC-CV charges

(b) Incremental Capacity curves

Fig. 3: CC-CV and IC curves for different levels of degradation

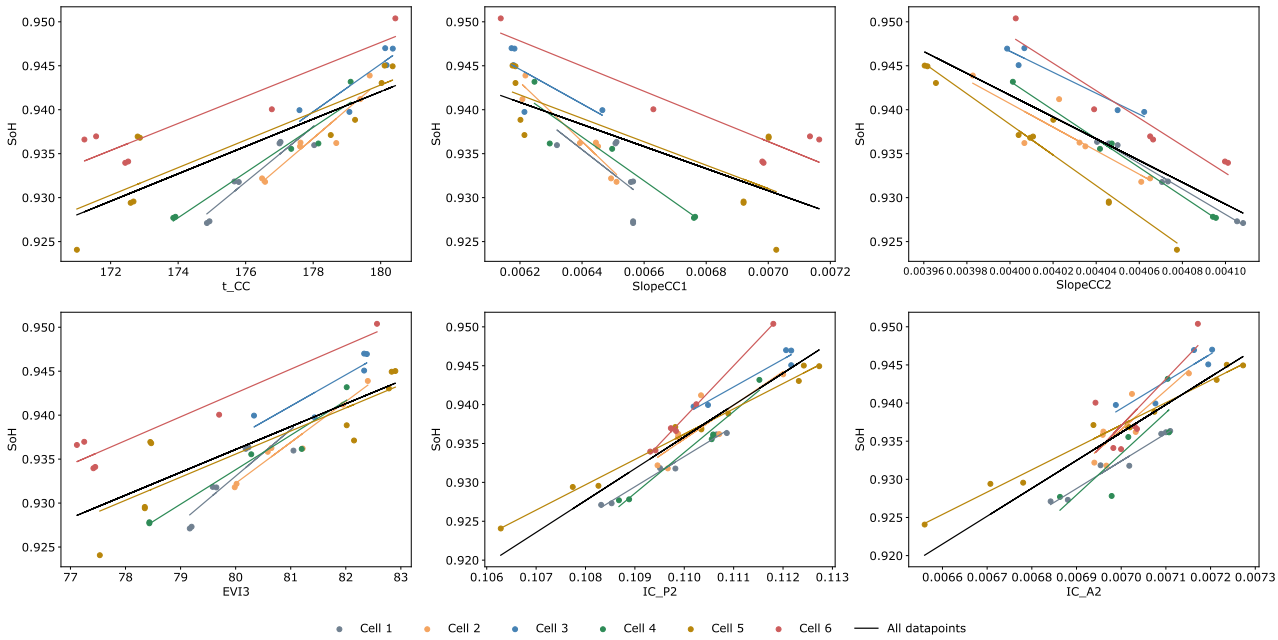

Fig. 4: Regression results for different HIs. *The markers represent the data points and the lines the linear regressions.*

earlier than the others. In the case of Cell 3, a 2% reduction in capacity leads to a 4% decline in SoF_e. Conversely, Cell 5 has the least restrictive capacity requirements, and its SoF_e only drops by 2% when the capacity decreases by 2%.

TABLE III: Errors for the different models

Model	MAE	MSE	$RMSE$
t_{CC}	2.64E-03	8.65E-06	2.94E-03
$SlopeCC_1$	3.26E-03	1.38E-05	3.71E-03
$SlopeCC_2$	3.38E-03	1.90E-05	4.36E-03
EVI_3	2.95E-03	1.05E-05	3.24E-03
IC_{P2}	2.45E-03	8.27E-06	2.88E-03
IC_{A2}	2.74E-03	9.96E-06	3.16E-03
$multiHIs$	1.64E-03	3.96E-06	1.99E-03

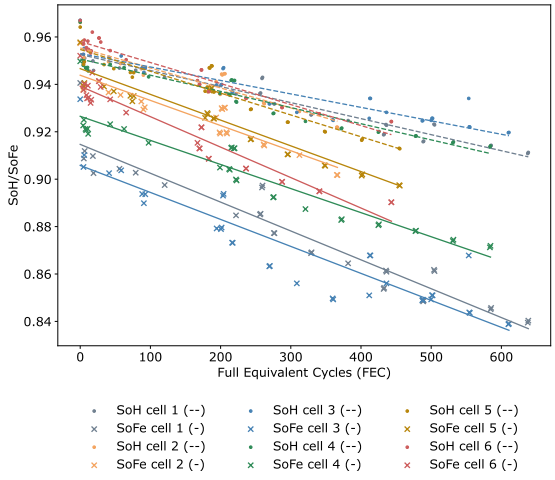

Fig. 5: SoH and SoF evolution for each cell. *The markers represent the data points and the lines the linear regressions.*

IV. Discussion

Section III has shown how different HIs can estimate the SoH using ideal full battery charges at constant conditions. However, in real life, charging periods vary and can affect the SoH estimation. EV charges are often incomplete, which affects the value of some HIs (i.e. t_{CC} and HIs obtained from IC curves) and makes some of them not even obtainable (slopes, EVI and IC related HIs obtained at specific voltage ranges). It is important to highlight that the shape of the IC curves is affected, and incomplete charges change the value and position of the peaks. In addition, current during charging may not remain constant due to charge point limitations, smart charging or Vehicle to Grid, affecting the voltage and peak measurements. Ambient temperature differences may also distort results as HIs are often obtained under constant temperature in laboratory conditions.

To address these issues, further analysis is required to define more realistic HIs. One possible approach is to redefine the EVIs or obtain HIs from partial IC curves based on common voltage ranges. In addition, considering the variability of working conditions, different algorithms can be built and when specific conditions are met that allow to accurately obtain one of the HIs, a particular algorithm can be executed to update the SoH. However, different HIs may provide more information than just the capacity fade. For instance, the movement of IC curves is influenced by the cycling history and reflects different degradation mechanisms [13]. To better represent battery health, the values of different HIs can be stored as a matrix. Additional analysis is required to understand the relationship between cycling conditions and HI evolution.

Section III has also highlighted the limitations of the current definition of SoH as an indicator of battery performance and

has introduced the concept of SoF_e as a more practical metric based on each driver's capacity requirements. However, for a more comprehensive analysis of battery functionality, other factors such as power capabilities need to be considered. The power capabilities of the battery depend on the degradation level and should be compared to the power requirements of the specific application. This will enable the prediction of the functional EoL point, beyond the capacity-based threshold. In fact, currently it is widely assumed that the EoL of the battery takes place when the capacity fades 20% regardless of the application requirements and nominal battery capacity [26]. The approach to define the SoF in this way, provides high value to increase the accuracy of the EoL and to extend the lifespan of the battery in the first life.

V. Conclusions

This work analyses experimental data representing diverse driving use cases to evaluate the applicability of different HIs to estimate the degradation and address the limitation of the SoH definition to represent the battery functionality.

Several HIs are obtained from full charges and their accuracy to estimate the SoH is compared. The value of the second IC peak shows the best correlation with the SoH. In addition, rather than using a single HI, the best estimation is obtained from combining several HIs. Nevertheless, further work is needed to find suitable HIs based on partial voltage ranges, representative of common usage patterns, and to evaluate the degradation mechanisms linked to each of them.

Additionally, the SoF has been used to provide a practical definition of the capacity fade. By analysing the driving requirements, the SoF is used to reflect how far the battery is from retirement, which is not observable through the SoH. The SoF allows to consider practical limitations of each application rather than assuming a fixed EoL for all cases.

Acknowledgment

This project has received funding from the European Union's Horizon 2020 research and innovation program under grant agreement No. 963580.

Lluc Canals Casals is a Serra Hunter Fellow.

References

[1] International Energy Agency (IEA), "Global Electric Vehicle Outlook 2022," Tech. Rep., 2022. [Online]. Available: https://www.iea.org/reports/global-ev-outlook-2022

[2] P. G. Pereirinha, M. González, I. Carrilero, D. Anseán, J. Alonso, and J. C. Viera, "Main Trends and Challenges in Road Transportation Electrification," *Transportation Research Procedia*, vol. 33, pp. 235–242, 2018.

[3] N. Rietmann, B. Hügler, and T. Lieven, "Forecasting the trajectory of electric vehicle sales and the consequences for worldwide CO2 emissions," *Journal of Cleaner Production*, vol. 261, p. 121038, Jul. 2020.

[4] J. Vetter, P. Novák, M. Wagner, C. Veit, K.-C. Möller, J. Besenhard, M. Winter, M. Wohlfahrt-Mehrens, C. Vogler, and A. Hammouche, "Ageing mechanisms in lithium-ion batteries," *Journal of Power Sources*, vol. 147, no. 1-2, pp. 269–281, Sep. 2005.

[5] R. Xiong, L. Li, and J. Tian, "Towards a smarter battery management system: A critical review on battery state of health monitoring methods," *Journal of Power Sources*, vol. 405, pp. 18–29, Nov. 2018.

[6] "On the feature selection for battery state of health estimation based on charging–discharging profiles," vol. 33.

[7] N. Williard, W. He, M. Osterman, and M. Pecht, "Comparative Analysis of Features for Determining State of Health in Lithium-Ion Batteries," *International Journal of Prognostics and Health Management*, vol. 4, no. 1, Oct. 2020.

[8] Y. Wu, Q. Xue, J. Shen, Z. Lei, Z. Chen, and Y. Liu, "State of Health Estimation for Lithium-Ion Batteries Based on Healthy Features and Long Short-Term Memory," *IEEE Access*, vol. 8, pp. 28 533–28 547, 2020.

[9] Y. Ma, C. Shan, J. Gao, and H. Chen, "A novel method for state of health estimation of lithium-ion batteries based on improved LSTM and health indicators extraction," *Energy*, vol. 251, p. 123973, Jul. 2022.

[10] D. Gong, Y. Gao, Y. Kou, and Y. Wang, "State of health estimation for lithium-ion battery based on energy features," *Energy*, vol. 257, p. 124812, Oct. 2022.

[11] D. Lin, X. Zhang, L. Wang, and B. Zhao, "State of health estimation of lithium-ion batteries based on a novel indirect health indicator," *Energy Reports*, vol. 8, pp. 606–613, Aug. 2022.

[12] B. Gou, Y. Xu, and X. Feng, "An Ensemble Learning-Based Data-Driven Method for Online State-of-Health Estimation of Lithium-Ion Batteries," *IEEE Transactions on Transportation Electrification*, vol. 7, no. 2, pp. 422–436, Jun. 2021.

[13] M. Dubarry, V. Svoboda, R. Hwu, and B. Yann Liaw, "Incremental Capacity Analysis and Close-to-Equilibrium OCV Measurements to Quantify Capacity Fade in Commercial Rechargeable Lithium Batteries," *Electrochemical and Solid-State Letters*, vol. 9, no. 10, p. A454, 2006.

[14] C. Weng, Y. Cui, J. Sun, and H. Peng, "On-board state of health monitoring of lithium-ion batteries using incremental capacity analysis with support vector regression," *Journal of Power Sources*, vol. 235, pp. 36–44, Aug. 2013.

[15] B. Ospina Agudelo, W. Zamboni, F. Postiglione, and E. Monmasson, "Battery State-of-Health estimation based on multiple charge and discharge features," *Energy*, vol. 263, p. 125637, Jan. 2023.

[16] A. Fly and R. Chen, "Rate dependency of incremental capacity analysis (dQ/dV) as a diagnostic tool for lithium-ion batteries," *Journal of Energy Storage*, vol. 29, p. 101329, Jun. 2020.

[17] W. Liu and Y. Xu, "A Comprehensive Review of Health Indicators of Li-ion Battery for Online State of Health Estimation," in *2019 IEEE 3rd Conference on Energy Internet and Energy System Integration (EI2)*. Changsha, China: IEEE, Nov. 2019, pp. 1203–1208.

[18] L. Wang, C. Pan, L. Liu, Y. Cheng, and X. Zhao, "On-board state of health estimation of LiFePO4 battery pack through differential voltage analysis," *Applied Energy*, vol. 168, pp. 465–472, Apr. 2016.

[19] H. Ji, W. Zhang, X. Pan, M. Hua, Y. Chung, C. Shu, and L. Zhang, "State of health prediction model based on internal resistance," *International Journal of Energy Research*, vol. 44, no. 8, pp. 6502–6510, Jun. 2020.

[20] Y. Yang, J. Wen, Y. Shi, and J. Zeng, "State of Health Prediction of Lithium-Ion Batteries Based on the Discharge Voltage and Temperature," *Electronics*, vol. 10, no. 12, p. 1497, Jun. 2021.

[21] L. Canals Casals, A. M. Schiffer Gonzalez, B. Garcia, and J. Llorca, "PHEV Battery Aging Study Using Voltage Recovery and Internal Resistance From Onboard Data," *IEEE Transactions on Vehicular Technology*, vol. 65, no. 6, pp. 4209–4216, Jun. 2016.

[22] I. Baghdadi, O. Briat, P. Gyan, and J. M. Vinassa, "State of health assessment for lithium batteries based on voltage–time relaxation measure," *Electrochimica Acta*, vol. 194, pp. 461–472, Mar. 2016.

[23] M. Etxandi-Santolaya, L. Canals Casals, and C. Corchero, "Estimation of electric vehicle battery capacity requirements based on synthetic cycles," *Transportation Research Part D: Transport and Environment*, vol. 114, p. 103545, Jan. 2023.

[24] M. Etxandi-Santolaya, L. Casals, and C. Corchero, "Redefining the EV Battery End of Life: Internal Resistance Related Limitations." Volume 26: Closing Carbon Cycles – A Transformation Process Involving Technology, Economy, and Society: Part I, Nov. 2022.

[25] M. Etxandi-Santolaya, L. Canals Casals, T. Montes, and C. Corchero, "Are electric vehicle batteries being underused? A review of current practices and sources of circularity," *Journal of Environmental Management*, vol. 338, p. 117814, Jul. 2023.

[26] L. Canals Casals, M. Rodríguez, C. Corchero, and R. E. Carrillo, "Evaluation of the End-of-Life of Electric Vehicle Batteries According to the State-of-Health," *World Electric Vehicle Journal*, vol. 10, no. 4, p. 63, Oct. 2019.